

# A Regional Assessment of OLCI Data Products

Giuseppe Zibordi<sup>1</sup>, Frédéric Mélin, and Jean-François Berthon

**Abstract**—This letter summarizes a regional assessment of radiometric data products from the Ocean and Land Colour Instrument operated onboard Sentinel-3A. The assessment is supported by *in situ* reference measurements from the Ocean Colour component of the Aerosol Robotic Network and the Bio-optical mapping of Marine Properties Program. Results indicate a systematic underestimate of the water-leaving radiance at the blue and red spectral bands. Conversely, the aerosol optical depth at 865 nm exhibits overestimate, while the Ångström exponent shows a narrow distribution of values confined below a maximum of approximately 1.7. These findings suggest difficulty in separating water and atmospheric radiance contributions, which results in a poor determination of aerosol load and type and, consequently, an overestimate of atmospheric effects.

**Index Terms**—Ocean colour, remote sensing, validation.

## I. INTRODUCTION

SATELLITE ocean colour data provide the capability to globally map the optically significant materials suspended or dissolved in natural waters. Among these, the concentration of chlorophyll-*a* (Chla) is a proxy for phytoplankton biomass commonly supporting environmental and climate investigations.

Chla, as any ocean colour geophysical product, is quantified from the normalized water-leaving radiance  $L_{WN}$  determined at key spectral bands in the visible and near-infrared (NIR) from the top-of-atmosphere radiance corrected for the atmospheric perturbations. The assessment of  $L_{WN}$  is thus a fundamental need for any satellite ocean colour mission in view of verifying the capability to meet the uncertainty requirements.

This letter focuses on reduced resolution (RR) data from the Ocean and Land Colour Instrument (OLCI). Providing continuity to the Medium Resolution Imaging Spectrometer (MERIS), OLCI has been operated onboard Sentinel-3A since February 2016 in the framework of the European Copernicus Program. It has also been active on Sentinel-3B since April 2018 and will be included in the payload of the following Sentinel-3C and Sentinel-3D missions.

The objective of this letter is an assessment of the accuracy of Level-2 ocean colour radiometric products from the Operational Processing Baseline 2.23 applied to OLCI 1.2-km resolution data from April 2016 to November 2017 [1], [2].

Manuscript received April 28, 2018; revised May 28, 2018 and June 18, 2018; accepted June 18, 2018. Date of publication August 6, 2018; date of current version September 26, 2018. This work was supported by the Joint Research Centre through the Earth Observation Support to Copernicus Climate and Marine Services activity. (Corresponding author: Giuseppe Zibordi.)

The authors are with the Joint Research Centre of the European Commission, 21027 Ispra, Italy (e-mail: giuseppe.zibordi@ec.europa.eu; frederic.melin@ec.europa.eu; jean-francois.berthon@ec.europa.eu).

Digital Object Identifier 10.1109/LGRS.2018.2849329

## II. DATA AND METHODS

The validation results presented in this letter were obtained from matchups (i.e., quasi-coincident *in situ* and satellite data) constructed with a maximum time difference  $\Delta T$  between *in situ* measurements and satellite overpass. Consistently with previous analysis [3], satellite RR data were retained for matchup construction when all the  $3 \times 3$  image elements centered at the *in situ* measurement locations satisfied the following criteria: 1) data were not affected by cloud contamination and, in general, by any of the main exclusion flags [2]; 2) the satellite viewing angle  $\theta$  was lower than  $56^\circ$  and the sun zenith angle  $\theta_0$  lower than  $70^\circ$ ; 3) the coefficients of variation of both  $L_{WN}$  at 555 nm and aerosol optical depth  $\tau_a$  at 865 nm were lower than 0.2.

The matchup analysis was separately performed for different marine regions to investigate differences between *in situ* and satellite data exhibiting diverse dynamics in the radiometric signal as a function of different optical properties of the water.

The comparison results are summarized through: 1) the median of relative (signed) percent differences  $\psi_m$  between remote sensing and *in situ* data (as an index for biases) and 2) the median of absolute (unsigned) percent differences  $|\psi|_m$  (as an index for dispersion). Additional statistical quantities provided to better support the data analysis are the root mean square of differences (rmsd) (with the same units of the quantity considered) and the coefficient of determination  $r^2$ .

### A. Satellite Data

The OLCI  $L_{WN}$  data,  $L_{WN}^{OLCI}$ , assessed in this letter were computed from the spectral reflectance  $\rho^{OLCI}$  included in the standard Level-2 products according to

$$L_{WN}^{OLCI} = \rho^{OLCI} \frac{E_0}{\pi} C_{f/Q} \quad (1)$$

where  $E_0$  is the mean extraterrestrial solar irradiance [4] and  $C_{f/Q}$  accounts for the bidirectional effects [2], [5].

In agreement with the previous studies [3], additional products assessed in this letter are  $\tau_a$  at 865 nm and the Ångström exponent  $\alpha$  determined in the NIR from the top-of-atmosphere radiances at 779 and 865 nm. Finally, OLCI Chla (i.e., *Algal-1* proposed for Case-1 and *Algal-2* for optically complex waters), is also matter of comparisons with *in situ* reference data.

### B. In Situ Data

The *in situ* data applied in this analysis, which are assumed to represent the atmospheric and marine optical properties of a number of European marine regions, are from: 1) the Ocean Colour component of the Aerosol Robotic Network (AERONET-OC) of autonomous radiometers operated at a number of coastal sites [3] and 2) the Bio-optical mapping of

Marine Properties (BioMaP) program ensuring the collection of comprehensive shipborne measurements across the various European seas [5].

The atmospheric and marine AERONET-OC data (i.e.,  $L_{WN}$ ,  $\tau_a$ , and  $\alpha$ ) are restricted to the Level-2 products exhibiting the highest level of quality assurance [3] and are confined to five European sites that include the Acqua Alta Oceanographic Tower (AAOT), also called Venise, in the northern Adriatic Sea representative of moderately sediment-dominated waters; Galata (GLT) and Gloria (GLR) in the Western Black Sea embracing waters dominated by variable concentrations of sediments and coloured dissolved organic matter (CDOM); and, finally, the Gustaf Dalen (GDLT) and the Helsinki (HLT) Lighthouses in the Baltic Proper and in the Gulf of Finland, respectively, representative of highly CDOM-dominated waters. The aerosol type is mostly continental with maritime influence at all the sites [6].

The BioMaP data (i.e.,  $L_{WN}$  and Chla) were collected during three oceanographic campaigns performed in: 1) the Western Black Sea (BLKS) onboard the R/V Akademik during June 2016; 2) the central Mediterranean Sea (EMED) onboard the R/V Minerva-1 during May 2017; and 3) the Iberian Shelf (ISHL) onboard the R/V A.G. Coutinho during September 2017. The aerosol type is continental with maritime influence in the BLKS, maritime with continental influences from various sources in the EMED, and maritime in the ISHL [7].

Uncertainties affecting *in situ*  $L_{WN}$  data significantly vary from region to region because of the different measurement methods, optical systems, illumination conditions, and water type. Specifically, the BioMaP  $L_{WN}$  applied in this letter were produced with a free-fall profiler and are expected to exhibit uncertainties generally lower than 5% in the blue–green spectral regions and slightly higher in the red [5]. Conversely, the AERONET-OC  $L_{WN}$  determined through above-water radiometry over very different water types is likely affected by uncertainties largely varying across the various regions with values close to 5% in the blue–green and reaching 8% in the red for the AAOT site but approaching 30% in the blue at the HLT site [8]. These differences are explained by the choice to quantify uncertainties in relative terms (i.e., in %) and by the very diverse range of  $L_{WN}$  characterizing the waters of the various marine regions. For instance, the median of  $L_{WN}$  measured at the AAOT in the blue is approximately one order of magnitude higher than that from the HLT values [8].

It is mentioned that the *in situ*  $L_{WN}$  applied in the analysis, for each site restricted to the measurements closer in time to the satellite overpass, were band-shifted [5] to match the OLCI center wavelengths and, consequently, minimize the impact of differences between equivalent spectral bands.

As already anticipated, the values of  $\alpha$  for OLCI are determined from NIR bands (i.e., those centered at 779 and 865 nm). Considering the available AERONET-OC bands, the *in situ* values of  $\alpha$  were determined from  $\tau_a$  at 665 and 870 nm.

With reference to Chla data, the *in situ* values were determined through High-Precision Liquid Chromatography applied to field samples. The uncertainty affecting these values is lower

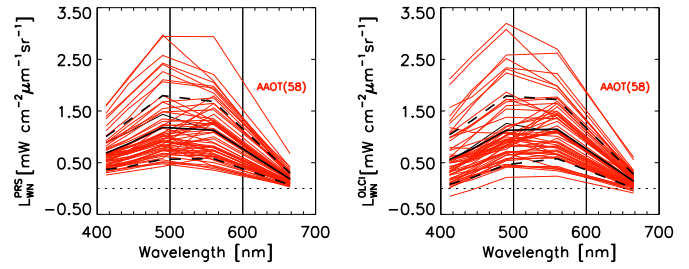


Fig. 1. (Left) *In situ*  $L_{WN}^{PRS}$  and (Right) satellite  $L_{WN}^{OLCI}$  spectra for the AAOT matchups (their number is given in brackets). The black continuous lines indicate the spectral averages and the black dashed lines indicate  $\pm 1$  std.

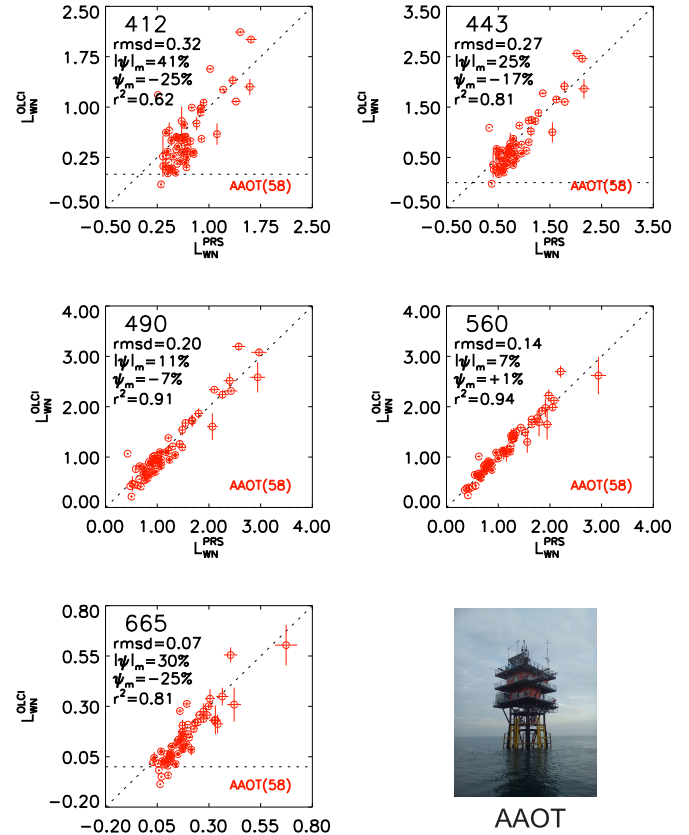


Fig. 2. Scatter plots of the AAOT  $L_{WN}^{OLCI}$  versus  $L_{WN}^{PRS}$  matchup values at 412, 443, 490, 560, and 665 nm. Axes and rmsd are in  $\text{mW} \cdot \text{cm}^{-2} \cdot \mu\text{m}^{-1} \cdot \text{sr}^{-1}$ . The semifilled symbols indicate the OLCI data not affected by the ANNOT flags. The error bars on the abscissa indicate the *in situ* measurement uncertainties. Conversely, on the ordinate, they indicate the variation coefficients of the  $3 \times 3$  OLCI elements. The picture illustrates the AAOT infrastructure hosting the AERONET-OC site.

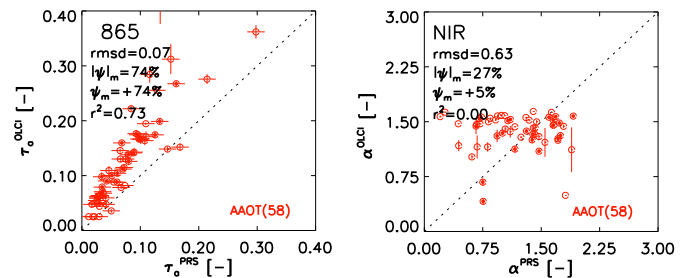


Fig. 3. Scatter plots of (Left)  $\tau_a^{OLCI}$  versus  $\tau_a^{PRS}$  at 865 nm and (Right)  $\alpha^{OLCI}$  and  $\alpha^{PRS}$  at the AAOT. Symbols are the same as in Fig. 2.

than 10% [5]. It is lastly reminded that the uncertainty assigned to  $\tau_a$  is 0.01 [9].

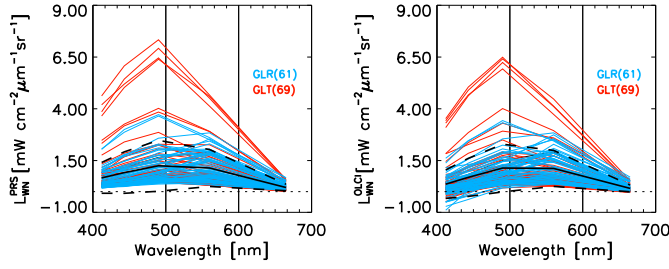


Fig. 4. As in Fig. 1, but for the GLT and GLR matchups. Colours identify data from different sites.

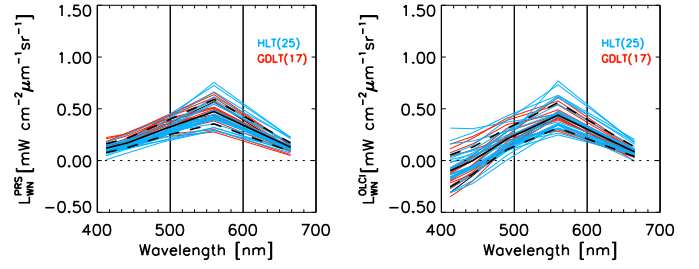


Fig. 7. As in Fig. 1, but for the GLDT and HLT matchups. Colours identify data from different sites.

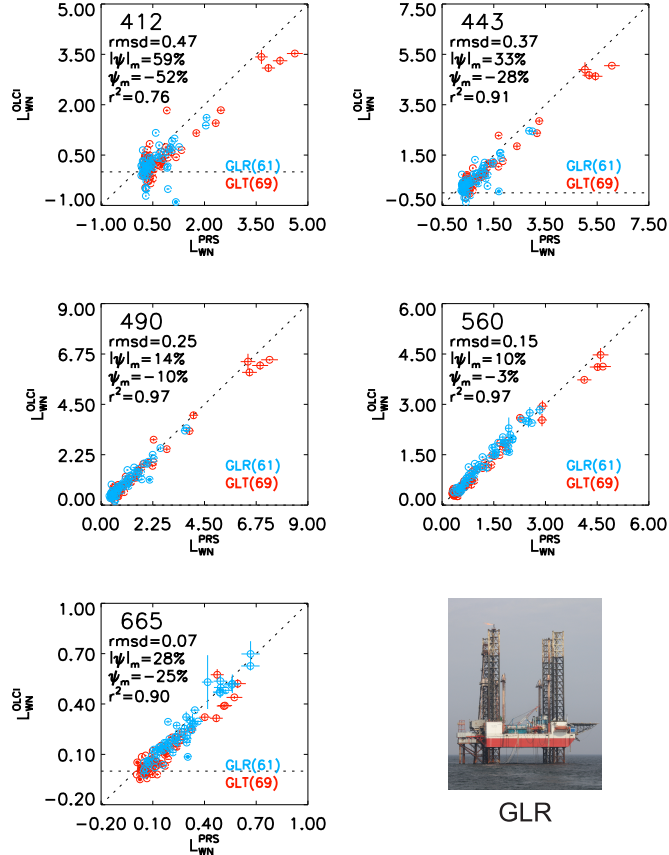


Fig. 5. As in Fig. 2, but for the GLT and GLR matchups. The picture illustrates the GLR infrastructure hosting the AERONET-OC site. Colours identify data from different sites.

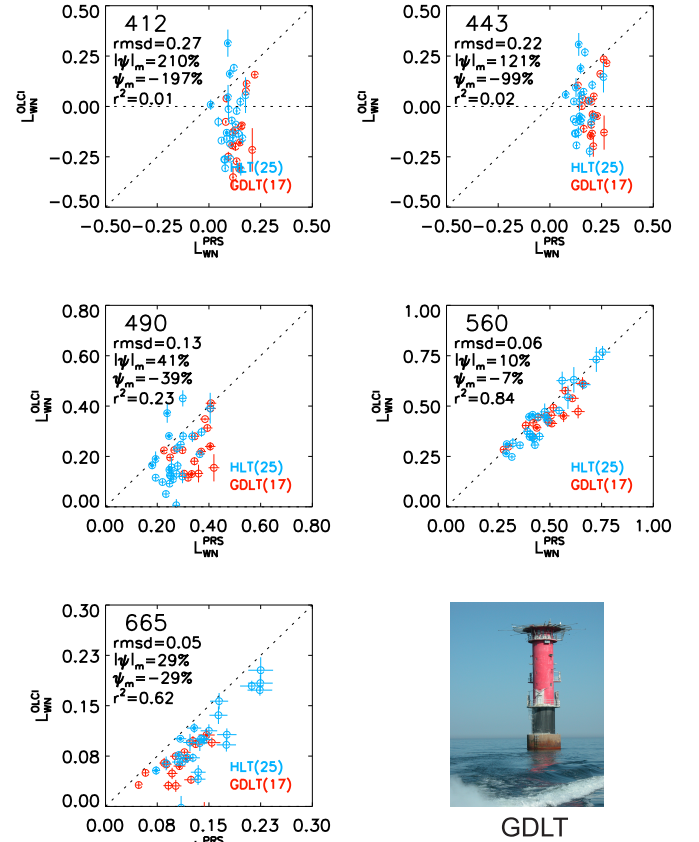


Fig. 8. As in Fig. 2, but for the GLDT and HLT matchups. The picture illustrates the GLDT infrastructure hosting the AERONET-OC site. Colours identify data from different sites.

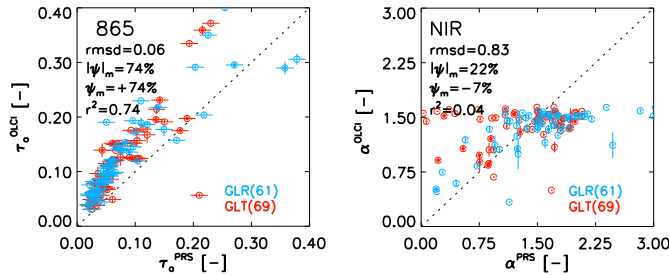


Fig. 6. As in Fig. 3, but for the GLT and GLR matchups. Colours identify data from different sites.

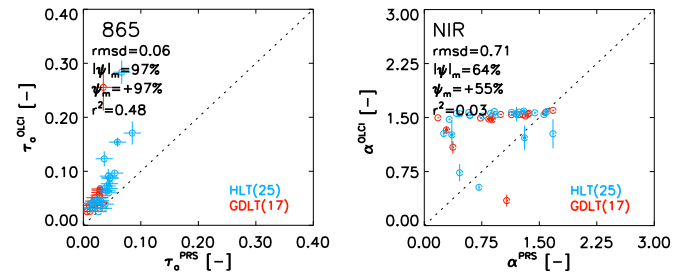


Fig. 9. As in Fig. 3, but for the GLDT and HLT matchups. Colours identify data from different sites.

### III. RESULTS AND DISCUSSION

Results are presented in Figs. 1–11 through the intercomparison of  $L_{WN}$ ,  $\tau_a$  at 865 nm, and  $\alpha$ . It is anticipated that the analysis related to Chla is presented solely for the BioMaP matchups in Fig. 12.

The matchups of *in situ* and satellite data were constructed applying a maximum time difference  $\Delta T$  of  $\pm 2$  hr for AERONET-OC data and  $\pm 4$  hr for BioMaP data. Still, for AERONET-OC matchups, more than 70% of the time



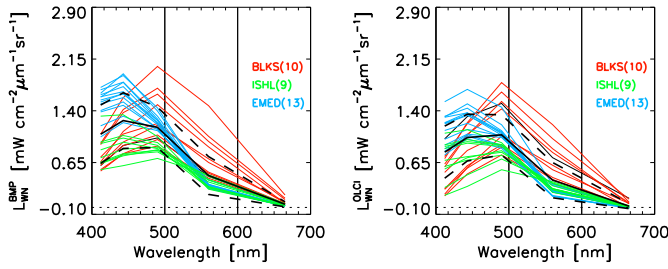


Fig. 10. As in Fig. 1, but for the EMED, IHSL and BLKS matchups. Colours identify data from different marine regions.

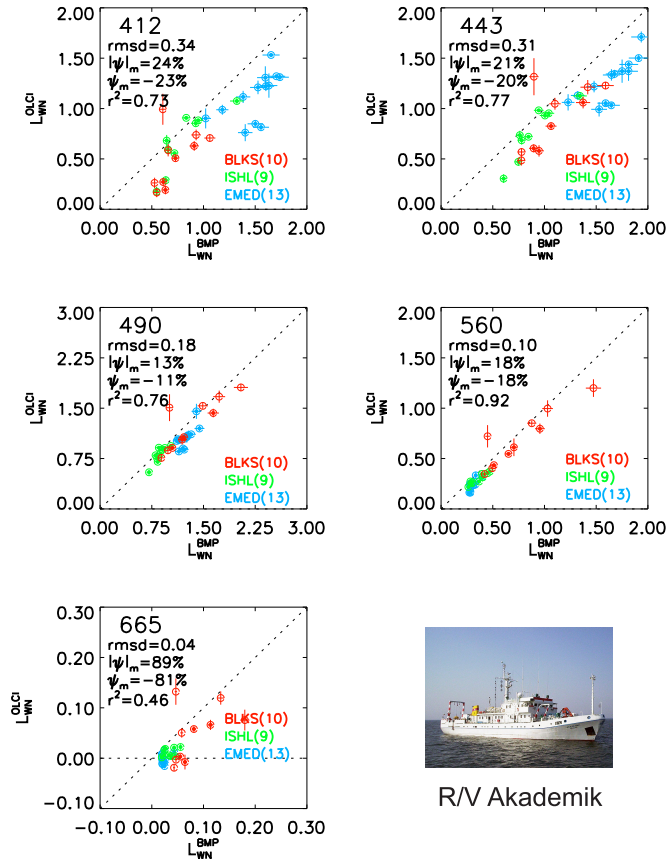


Fig. 11. As in Fig. 2, but for the EMED, IHSL and BLKS matchups. The picture illustrates the R/V Akademik. Colours identify data from different marine regions.

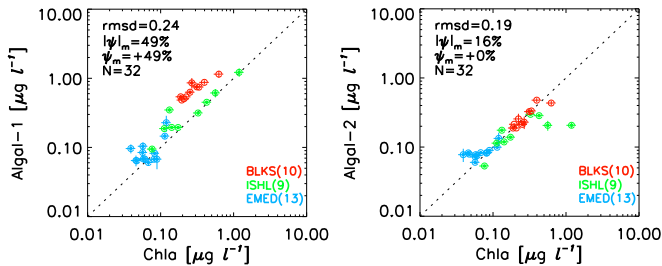


Fig. 12. Scatter of OLCI derived pigments concentration [i.e., (Left) *Algal-1* and (Right) *Algal-2*] versus *in situ* BioMaP Chla determined for the EMED, IHSL, and BLKS marine regions. Colours identify data from different marine regions.

differences were within  $\pm 1$  hr, and for BioMaP, approximately 50% were within  $\pm 2$  hr.

The so-called ANNOT flags provided with OLCI data products [2] and recommended for validation exercises were

not accounted for in the construction of matchups. In fact, while they do not have any significant impact on the analysis of data from open sea regions, such as EMED and IHSL, they may lead to the exclusion of a large number of *in situ*—satellite matchups (i.e., from 60% to 90%) from optically complex regions mostly associated with relatively high values of  $L_{WN}$ . Still, for the sake of completeness, these matchups are identified by open circles in the scatter plots.

For convenience, the figures illustrating the comparisons are organized by grouping the AERONET-OC data products according to the various marine regions (i.e., the Adriatic Sea, the Black Sea, and the Baltic Sea) and, conversely, by combining all the BioMaP data regardless of the marine region.

#### A. Normalized Water-Leaving Radiance

The qualitative comparison of *in situ* and satellite  $L_{WN}$  spectra, restricted to the bands for which *in situ* data exist (i.e., those identified by the center wavelengths at 412, 443, 490, 560, and 665 nm), are presented in Figs. 1, 4, 7, and 10. The main purpose of such a comparison is to illustrate the type of spectra included in the analysis and show artifacts that may characterize either satellite or *in situ* data.

The spectra in Figs. 1, 4, 7, and 10 indicate a fair qualitative agreement between *in situ* and satellite spectra. Still, striking is the presence of negative  $L_{WN}$  affecting OLCI data in the blue spectral bands at the HLT and GDLT sites [see Fig. 7 (right)]. This feature, however, should be considered in the context of the very low values of  $L_{WN}$  characterizing the Baltic Sea data in the blue spectral region.

Remarkable are also the high radiance values characterizing a few  $L_{WN}$  spectra from GLT (see Fig. 4). These spectra, noticeable for both *in situ* and satellite data, were acquired on June 2017 during an exceptional coccolithophores bloom that mostly developed in the southern part of the western Black Sea (i.e., where the GLT site is located).

Quantitative comparisons between satellite and *in situ* data are presented in Figs. 2, 5, 8, and 11 through individual scatter plots for each spectral band. Notably, the AAOT data in Fig. 2 and the BioMaP data in Fig. 11 do not show any significant impact of negative radiances at the blue bands (just one single-AAOT matchup exhibits a negative value for OLCI at 412 nm). However, high occurrence of OLCI negative  $L_{WN}$  data is observed in Fig. 5 for GLT and GLR in the Black Sea. Specifically, negative  $L_{WN}$  appear at 412, 443, and 665 nm. An analysis restricted to the spectra exhibiting those negative radiances showed that they mostly pertain to CDOM-dominated waters (i.e., exhibiting  $L_{WN}$  spectra with maxima at 560 nm and relative minima at 412 and 665 nm). This finding is fully supported by the scatter plots shown in Fig. 8 for GDLT and HLT. Still, regardless of the water type, it is expected that the negative  $L_{WN}$  often observed in the Baltic and Black Seas are the result of an overcorrection of the atmospheric effects. This interpretation is supported by the similarity observed among the scatter plots of  $\tau_a$  and  $\alpha$  proposed for the different marine regions (see Section III-B).

The rmsd values determined from the OLCI  $L_{WN}$  matchups vary from 0.3–0.5  $\text{mW} \cdot \text{cm}^{-2} \cdot \mu\text{m}^{-1} \cdot \text{sr}^{-1}$  at 412 nm,

0.2–0.4 at 443 nm, decrease to 0.1–0.2 at 490 and 560 nm, and finally exhibit values lower than 0.1 at 665 nm. An evaluation of biases through  $\psi_m$  indicates values largely varying with the amplitude of  $L_{WN}$  with minima generally within a few percent at 560 nm except for the BioMaP matchups.

Overall results from the analysis of  $L_{WN}$  indicate large equivalence with findings from the assessment of MERIS Level-2 data from the third reprocessing [10].

### B. Aerosol Optical Depth

The aerosol products  $\tau_a$  and  $\alpha$ , which are the by-products of the atmospheric correction, may likely provide insight on the correction process or the calibration accuracy of the NIR bands applied to determine the aerosol type. Comparisons between satellite and *in situ* atmospheric products are illustrated in Figs. 3, 6, and 9. Results show a systematic overestimate that generally exceeds 70% for OLCI  $\tau_a$  at 865 nm. Notably, the values of  $\alpha$  from OLCI do not exhibit any correlation with the *in situ* values and show a very narrow distribution below a maximum of approximately 1.7. This indicates issues in the accurate determination of the aerosol type.

### C. Seawater Constituents

The analysis of seawater constituents is centered on Chla for the 32 BioMaP matchup stations. Results in Fig. 12 indicate some systematic overestimate of *Algal-1* data for the Mediterranean Sea oligotrophic waters and for the optically complex waters of the Black Sea. Excluding some matchups from the Iberian Shelf and Mediterranean regions, the *Algal-2* data, which result from an alternative processing [2], exhibit much better agreement. Still, the relatively limited number of matchups prevent considering this comparison as a consolidated assessment of OLCI pigments concentrations for the current processing.

## IV. CONCLUSION

The comparisons between OLCI and *in situ* normalized water-leaving radiances  $L_{WN}$  indicate the systematic underestimates of satellite radiometric products with effects more pronounced in the blue and red spectral regions. While the OLCI aerosol optical depths  $\tau_a$  at 865 nm resulting from the atmospheric correction process indicate the systematic overestimates, the OLCI-derived Ångström exponents  $\alpha$  exhibit a very narrow distribution close to a maximum value of approximately 1.7. These findings indicate difficulty in separating water and atmospheric radiance contributions likely explained by biases in calibration coefficients or low performance of the

bright pixel correction, which results in a poor determination of aerosol load and type, and a consequent systematic overestimate of atmospheric effects.

## ACKNOWLEDGMENT

The authors would like to thank EUMETSAT for providing the Ocean and Land Colour Instrument (OLCI) Level 2 data and the AERONET Team for processing and distributing the data from the Ocean Colour component of the Aerosol Robotic Network. They would also like to thank the Institute of Oceanology, Varna, Bulgaria, for providing access to the R/V Akademik, the Institute of Atmospheric and Climate Science, Rome, Italy, for providing access to the R/V Minerva-1, and the Portuguese Hydrographic Institute, Lisbon, Portugal, for providing access to the R/V A.G. Coutinho.

## REFERENCES

- [1] EUMETSAT. (2018). Sentinel-3A product notice—OLCI Level-2 ocean colour operational products and full-mission reprocessed time series. Product Notice EUM/OPS-SEN3/DOC/17/964713. [Online]. Available: [https://www.eumetsat.int/website/wcm/idc/idcplg?IdcService=GET\\_FILE&dDocName=PDF\\_S3A\\_PN\\_OLCI\\_L2\\_REP&RevisionSelectionMethod=LatestReleased&Rendition=Web](https://www.eumetsat.int/website/wcm/idc/idcplg?IdcService=GET_FILE&dDocName=PDF_S3A_PN_OLCI_L2_REP&RevisionSelectionMethod=LatestReleased&Rendition=Web)
- [2] EUMETSAT. (2018). Sentinel-3 OLCI marine user handbook. EUM/OPS-SEN3/MAN/17/907205. [Online]. Available: [http://www.eumetsat.int/website/wcm/idc/idcplg?IdcService=GET\\_FILE&dDocName=PDF\\_DMT\\_907205&RevisionSelectionMethod=LatestReleased&Rendition=Web](http://www.eumetsat.int/website/wcm/idc/idcplg?IdcService=GET_FILE&dDocName=PDF_DMT_907205&RevisionSelectionMethod=LatestReleased&Rendition=Web)
- [3] G. Zibordi, J. F. Berthon, F. Mélin, D. D'Alimonte, and S. Kaitala, "Validation of satellite ocean color primary products at optically complex coastal sites: Northern Adriatic Sea, Northern Baltic Proper and Gulf of Finland," *Remote Sens. Environ.*, vol. 113, no. 12, pp. 2574–2591, 2009.
- [4] G. Thuillier *et al.*, "The solar spectral irradiance from 200 to 2400 nm as measured by the SOLSPEC spectrometer from the atlas and Eureca missions," *Solar Phys.*, vol. 214, no. 1, pp. 1–22, 2003.
- [5] G. Zibordi, J.-F. Berthon, F. Mélin, and D. D'Alimonte, "Cross-site consistent *in situ* measurements for satellite ocean color applications: The BioMaP radiometric dataset," *Remote Sens. Environ.*, vol. 115, no. 8, pp. 2104–2115, 2011.
- [6] F. Mélin, G. Zibordi, T. Carlund, B. N. Holben, and S. Stefan, "Validation of SeaWiFS and MODIS Aqua/Terra aerosol products in coastal regions of European marginal seas," *Oceanologia*, vol. 55, no. 1, pp. 27–51, 2013.
- [7] F. Mélin, M. Clerici, G. Zibordi, B. N. Holben, and A. Smirnov, "Validation of SeaWiFS and MODIS aerosol products with globally distributed AERONET data," *Remote Sens. Environ.*, vol. 114, no. 2, pp. 230–250, 2010.
- [8] M. M. Gergely and G. Zibordi, "Assessment of AERONET-OC  $L_{WN}$  uncertainties," *Metrologia*, vol. 51, no. 1, pp. 40–47, 2013.
- [9] T. F. Eck *et al.*, "Wavelength dependence of the optical depth of biomass burning, urban, and desert dust aerosols," *J. Geophys. Res.*, vol. 104, no. D24, pp. 31333–31350, 1999.
- [10] G. Zibordi, F. Mélin, J.-F. Berthon, and E. Canuti, "Assessment of MERIS ocean color data products for European seas," *Ocean Sci.*, vol. 9, pp. 521–533, May 2013.